ISSN: 2277-3754
ISO 9001:2008 Certified
International Journal of Engineering and Innovative Technology (IJEIT)
Volume 4, Issue 6, December 2014

PAPR Reduction using DFT Spread Technique for Nonlinear Communication Systems

Shatrughna Prasad Yadav, Subhash Chandra Bera
Electrical and Electronics Engineering Department, Indus University, Ahmedabad
Satcom & Navigation Systems Engineering Division, Space Applications Centre, Indian Space Research Organization, Ahmedabad

Abstract*—Discrete Fourier Transform (DFT) spread is a modified form of orthogonal frequency division multiplexing (OFDM) system. It promises high data rate for uplink communications with lower peak to average power ratio (PAPR) than the conventional OFDM system. It has similar throughput performance and structural complexity as OFDM. In the present work PAPR performance analysis has been done for its different subcarrier mapping approaches. Among the localized FDMA (LFDMA), distributed FDMA (DFDMA) and interleaved FDMA (IFDMA) the PAPR performance of IFDMA has been found to be better than that of DFDMA and LFDMA. When the DFD spreaded signals are passed through a raised cosine pulse shaping filer IFDMA system shows sharp reduction in PAPR with increase in roll-off factor from 0 to 1. The response of LFDMA is not that much affected by the pulse shaping network. The PAPR performance of DFT - spread also depends on the number of subcarriers allocated to each user. The PAPR of LFDMA decreases with increase in number of subcarriers at a fixed value of roll-off factor. Even though PAPR value of IFDMA is lower than that of LFDMA, LFDMA is usually preferred than IFDMA from implementation point of view because subcarriers allocation with equal distance over the entire band in IFDMA is a difficult task.

***Index Terms*—Orthogonal frequency division multiplexing, Discrete Fourier Transform Spread, peak to average power ratio, localized FDMA, distributed FDMA, interleaved FDMA.**

I. INTRODUCTION

There is a constant demand of high data rate for the future cellular and local area wireless communications Systems. Orthogonal Frequency Division Multiplexing (OFDM) system promises to deliver highest bit rates in commercially deployed wireless systems based on the IEEE 802.11a and IEEE 802.11g standards. The future advances in cellular systems, like third generation partnership project (3GPP), uses orthogonal frequency division multiple accessing (OFDMA) to achieve higher bit rates. OFDMA is based on the orthogonal frequency-division multiplexing (OFDM) modulation technique. It is based on the principle of splitting the data stream into large number of narrowband subcarriers which are orthogonal to each other with an inverse discrete Fourier transform (IDFT) operation [1]. OFDM system has many advantages over traditional communication systems such as it uses simple receiver as it turns the frequency-selective fading channel into a flat fading channel, it is a spectrally efficient and is ideal for multimedia communications, and it has been widely accepted for future communication for different services. But it also suffers from the disadvantages, like sensitive to time and frequency synchronization errors, high value of peak-to-average power ratio (PAPR), inter carrier interference (ICI) and co-channel interference (CCI). Cyclic prefix (CP) is added at the beginning of each OFDM symbol which is a repetition of the last part of an OFDM symbol. If length of cyclic prefix is larger than the maximum delay of the channel, distortions due to intersymbol interference (ISI) and intercarrier interference (ICI) are avoided. The narrowband subcarriers also avoids frequency selective multipath fading and promises only flat fading response which makes equalization much simpler at the receiver. As, subcarriers are orthogonal to each other, overlapping between them can happen resulting in a highly spectral efficient system. DFT- spread, also known as single carrier (SC) FDMA, is a multiple access technique which is based on the single-carrier frequency-division multiplexing (SC-FDM) modulation technique. Its operation is based on the principle of OFDM [2]. Hence all the benefits in terms of multipath mitigation and low-complexity equalization are achieved. But DFT - spread differs from OFDM as DFT operation is performed prior to the IDFT operation resulting in spreading of the data symbols over entire subcarriers and results in a virtual single- carrier structure. The major advantage of DFT- spreading is having a lower PAPR than OFDM system. The lower value of PAPR makes it an attractive candidate for uplink transmissions, as it gives the benefit of transmitted power efficiency. It also allows the frequency selectivity of the channel as all symbols are present in all subcarriers. Information can still be recovered from other subcarriers experiencing better channel conditions if a particular subcarrier is deeply faded. It suffers from the disadvantage of noise enhancement as noise is spread over all the subcarriers when DFT despreading is done at the receiver [3].

II. DFT SPREAD TRANSCEIVER SYSTEMS

Like OFDM the transmitter of a DFT spread system consists of serial to parallel convertor, DFT spreading, IDFT operation, reconverting parallel data into serial form, adding cyclic prefix, using digital to analog convert and finally RF modulation for converting baseband signal into passband signal before transmitting through the channel [4].

ISSN: 2277-3754
ISO 9001:2008 Certified
International Journal of Engineering and Innovative Technology (IJEIT)
Volume 4, Issue 6, December 2014

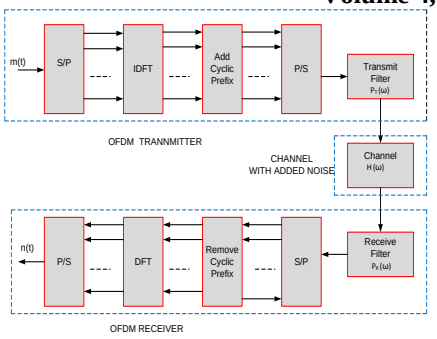

Fig 1 Block diagram of OFDM system

In the receiver, reverse process of transmitter is performed. Block diagram of OFDM and DFT spread is shown in figure and 1 and 2 respectively.

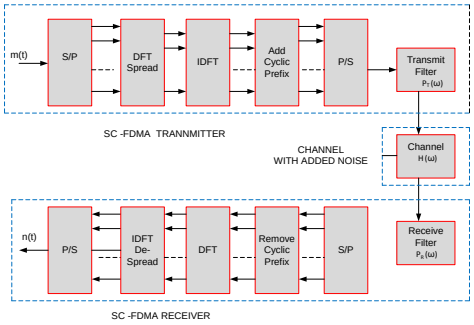

Fig 2 Block diagram of DFT spread system

If DFT of the same size as that of IDFT is used for spreading code then, the OFDMA system becomes equivalent to the single carrier FDMA (SC-FDMA) system because the DFT and IDFT operations virtually cancel each other. Then the transmit signal will have the same PAPR as in a single-carrier system [5]. The equivalence of OFDMA system with DFT-spreading to a single-carrier system is shown in figure 3.

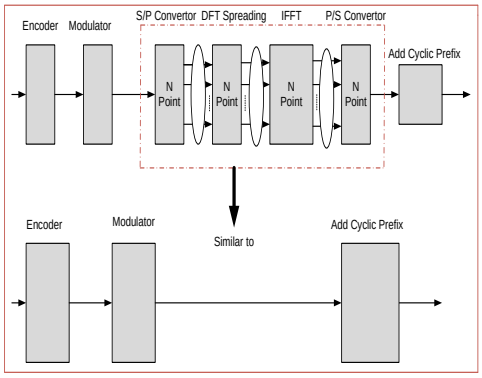

Fig 3 Equivalence of OFDMA systems with DFT-spread

In a conventional OFDMA system, subcarriers are partitioned and assigned to multiple mobile users. But in the DFT- spread technique which is used for the uplink transmission, each user uses a subset of subcarriers to transmit its own data. The subcarriers which are not used for the data transmission are filled with zeros [6].

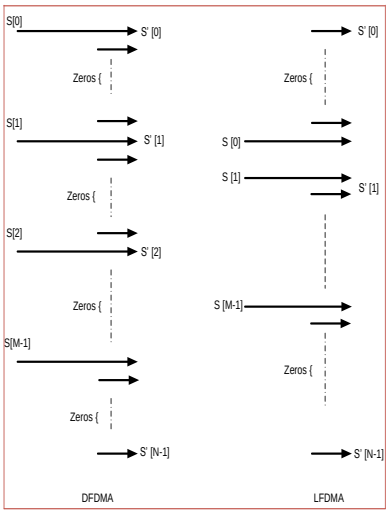

Fig 4 Sub carrier mapping for uplink in DFDMA and LFDMA.

Here, the number of subcarriers allocated to each user is assumed to be M. In the DFT-spreading technique, M-point DFT is used for spreading, and the output of DFT is assigned to the subcarriers of IDFT. The effect of PAPR reduction depends on the way of assigning the subcarriers to each terminal. Two different approaches of assigning subcarriers are used among users, DFDMA (Distributed FDMA) and LFDMA (Localized FDMA) as shown in figure 4. In DFDMA, M DFT outputs are distributed over the entire band of total N subcarriers with zeros filled in N-M unused subcarriers. But in the LFDMA, DFT outputs are allocated to M consecutive subcarriers in N subcarriers and remaining are filled with zeros. If distribution of DFT outputs in DFDMA is done uniformly with equal distance then it is referred to as Interleaved FDMA (IFDMA) [7].

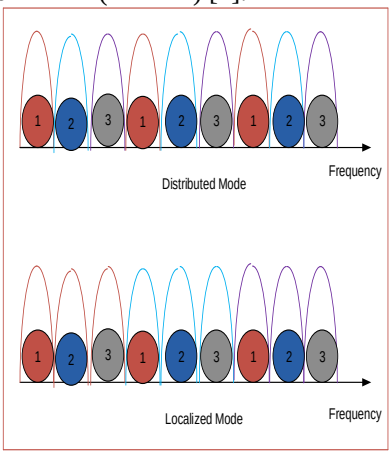

Fig 5 Subcarrier assignments to multiple users

Figure 5 illustrates the subcarrier allocation in the DFDMA and LFDMA with M =3, N = 9,V = 3, and, where V = N/M is called the bandwidth spreading factor. Figure 6 shows the examples of DFT spreading in DFDMA, LFDMA, and IFDMA with N = 9, M = 3, and V = 3. It illustrates a subcarrier mapping relationship between 3 -point DFT and 9 -point IDFT for three different types of DFT spreading techniques.

ISSN: 2277-3754
ISO 9001:2008 Certified
International Journal of Engineering and Innovative Technology (IJEIT)
Volume 4, Issue 6, December 2014

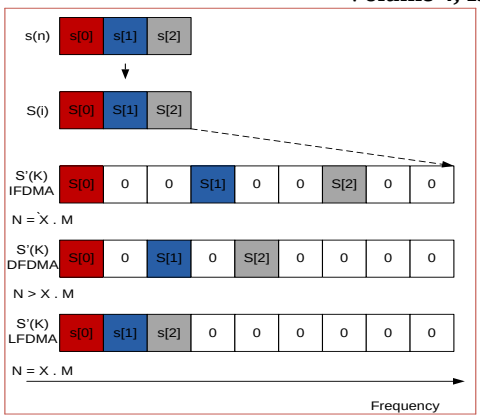

Fig 6 DFT spreading for IFDMA, FDMA and LFDMA

Block diagram of the uplink transmitter which employs the DFT-spreading technique in IFDMA is shown Figure 7. Input data s [m] is DFT-spread to generate S[k] signals in frequency domain as given in equation (1).

$$X_k = \sum_{k=0}^{N-1} S'[k] e^{-j2\Pi nk/N} \qquad (1)$$

These are allocated as depicted in equation (2).

$$S'[k] = \begin{cases} S\left[\frac{k}{X}\right], & k = X.\ m_1,\ \ m_1 = 0,1,2,3 \ldots\ldots, m-1 \\ 0\ , & otherwise \end{cases} \qquad (2)$$

The IFFT output sequence s'[n] with n = M . x + m for x = 0, 1, 2, ……. , X-1 and m = 0, 1, 2, ……. , M-1can be expressed as shown in equation (3).

$$s'[n] = \frac{1}{N}\sum_{k=0}^{N-1} S'[k] e^{j2\Pi nk/N}$$

$$= \frac{1}{X}\frac{1}{M}\sum_{m_1=0}^{M-1} S[m_1] e^{j2\Pi n m_1/M}$$

$$= \frac{1}{X}\frac{1}{M}\sum_{m_1=0}^{M-1} S[m_1] e^{\frac{j2\Pi (M_X+m).m_1}{M}}$$

$$= \frac{1}{X}\sum_{m_1=0}^{M-1}\frac{1}{M} S[m_1] e^{\frac{j2\Pi\, m.m_1}{M}}$$

$$= \frac{1}{X}\sum_{m_1=0}^{M-1} S[m] \qquad (3)$$

This is a repetition of the original input signal s[m] scaled by 1= X in the time domain.

For the IFDMA where the subcarrier mapping starts with the rth subcarrier (r = 0, 1, 2, …X-1), the DFT-spread symbol is expressed as in equation (4).

$$S'[k] = \begin{cases} S\left[\frac{k-r}{X}\right], k = X.\ m_1 + r, m_1 = 0,1,2, \ldots, m-1 \\ 0\ , \qquad otherwise \end{cases}$$

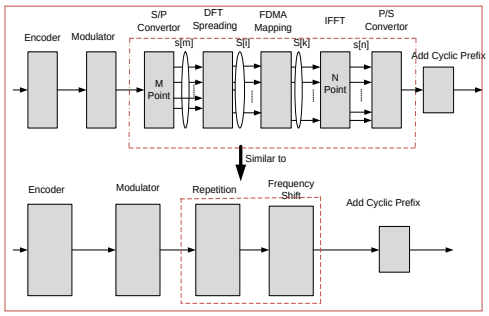

Fig 7 Uplink transmitters for IFDMA mapping

In this case the corresponding IFFT output sequence, {s'[n]}, is given by equation (5).

$$s[n] = s'[Mx+m]$$

$$= \frac{1}{N}\sum_{k=0}^{N-1} S'[k] e^{j2\Pi nk/M}$$

$$= \frac{1}{X}\frac{1}{M}\sum_{m_1=0}^{M-1} S[m_1] e^{j2\Pi\left(\frac{nm_1}{M}+\frac{nr}{N}\right)}$$

$$= \frac{1}{X}\frac{1}{M}\sum_{m_1=0}^{M-1} S[m_1] e^{j2\Pi\frac{(Mx+m)}{M}m_1} . e^{\frac{j2\Pi n}{N^r}}$$

$$= \frac{1}{X}\left(\frac{1}{M}\sum_{m_1=0}^{M-1} S[m_1] e^{\frac{j2\Pi\, m.m_1}{M}}\right) . e^{\frac{j2\Pi n}{N^r}}$$

$$= \frac{1}{X} . e^{\frac{j2\Pi n}{N^r}} . S[m] \qquad (5)$$

When it is compared with equation (3), it is evident that the frequency shift of subcarrier allocation starting point by r subcarriers gives a phase rotation of $e^{\frac{j2\Pi n}{N^r}}$ in IFDMA mapping. For LFDMA mapping, the IFFT input signal $S'[k]$ at the transmitter is expressed as in equation (6).

$$S'[k] = \begin{cases} S[k], & k = 0,1,2, \ldots\ldots, M-1 \\ 0\ , & k = M, M+1, \ldots\ldots, N-1 \end{cases} \qquad (6)$$

The IFFT sequence $s'[n]$ with n= X.m + x for x = 0,1,2,….X-1 is expressed as in equation (7).

$$s'[n] = s'[Xm+x] = \frac{1}{N}\sum_{k=0}^{N-1} S[k] e^{j2\Pi\frac{n}{N}k}$$

$$= \frac{1}{X}\frac{1}{M}\sum_{k=0}^{M-1} S[k] e^{j2\Pi\frac{(Xm+x)}{XM}k} \qquad (7)$$

When x= 0, equation (7) is represented as in equation (8).

$$s'[n] = s'[Xm] = \frac{1}{X}\frac{1}{M}\sum_{k=0}^{M-1} S[k] e^{j2\Pi\frac{(Xm)}{XM}k} \qquad (4)$$

ISSN: 2277-3754
ISO 9001:2008 Certified
International Journal of Engineering and Innovative Technology (IJEIT)
Volume 4, Issue 6, December 2014

$$= \frac{1}{X}\frac{1}{M}\sum_{k=0}^{M-1} S[k]e^{j2\pi\frac{m}{M}k}$$

$$= \frac{1}{X}\, s[m] \qquad (8)$$

But in the case of $x \neq 0$, it is represented as in equation (9).

$$S[k] = \sum_{p=0}^{M-1} S[p]e^{-j2\pi\frac{p}{M}k} \qquad (9)$$

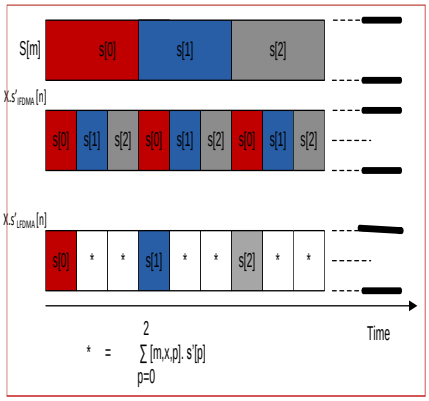

Fig 8 Time-domain signals for IFDMA and LFDMA

Then equation (7) changes and is represented by equation (10).

$$s'[n] = s'[Xm + x]$$

$$= \frac{1}{X}\left(1 - e^{j2\pi\frac{x}{X}}\right).\frac{1}{M}\sum_{p=0}^{M-1}\frac{s[p]}{1 - e^{j2\pi\left\{\frac{(m-p)}{M} + \frac{x}{XM}\right\}}}$$

$$= \frac{1}{X}\, e^{j\pi\frac{(M-1)x - Xm}{XM}}.\sum_{p=0}^{M-1}\frac{\sin\left(\Pi\frac{x}{X}\right)}{M\sin\left(\Pi.\frac{Xm+x}{XM} - \Pi\frac{p}{M}\right)}$$

$$.\left(e^{j\pi\frac{p}{M}}\, s[p]\right) \qquad (10)$$

It can be seen from Equations (8) and (10), that the time-domain LFDMA signal becomes the 1/X-scaled copies of the input sequence at the multiples of X in the time domain. Other values are calculated by adding all the input sequences with the different complex-weight factor. Time-domain signals when the DFT-spreading technique for IFDMA and LFDMA is applied with N = 9, M = 3, and X = 3, where $s'_{IFDMA}[n]$ and $s'_{LFDMA}[n]$ is shown in figure 8 which are expressed by Equations (5) and (10), respectively.

III. PAPR ANALYSIS OF DFT – SPREAD

In a conventional OFDM system PAPR is defined as the ratio of the maximum power and the average power of the complex passband signal as given in equation (11).

$$PAPR\{u(t)\} = \frac{max\ |[Re\{u(t)\}e^{j2\pi f_c t}\}]|^2}{E\{|[Re\{u(t)\}e^{j2\pi f_c t}\}]|^2}$$

$$= \frac{max\ |u(t)|^2}{E\{|u(t)|^2\}} \qquad (11)$$

Maximum peak power occurs when all the N subcarrier components are added with same phases and is a case of constructive addition [8]. Without pulse shaping, symbol rate sampling will gives the same PAPR as the continuous time domain case since an DFT - spread signal is modulated over a single carrier. Simulation of 6000 blocks of symbols have been done for Number of subcarriers varying from 256, 512 and 1024 for 4-QAM, 16-QAM and 64-QAM modulated signals [9]. Complementary cumulative distribution function (CCDF) is used to find out the probability that the PAPR exceeds a particular value z as given in equation (12).

$$F_{z_{max}}(z) = P(z_{max} < z)$$

$$= 1 - P(z_{max} \leq z)$$

$$= 1 - F_{z_{max}}(z)$$

$$= 1 - \left(1 - e^{-z^2}\right)^N \qquad (12)$$

Comparison of PAPR performances is shown in figure 9 when the DFT-spreading technique is applied to the IFDMA, LFDMA, and OFDMA [10].

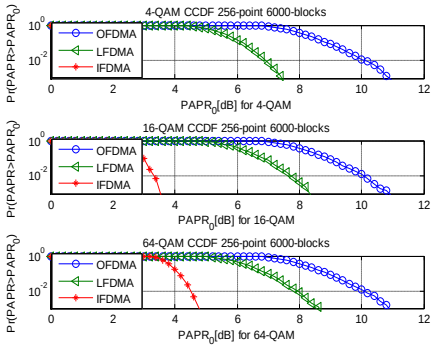

Fig 9 PAPR performances for IFDMA, LFDMA, and OFDMA for N= 256

Different modulation techniques like, 4-QAM, 16-QAM and 64 QAM signals are used for DFT - spread system with N =256, M = 64, and V = 4. It can be observed from figure 9 that the PAPR performance of the DFT-spread technique varies as per the subcarrier allocation method [11]. For the case of 16-QAM modulated signal, the values of PAPRs with IFDMA, LFDMA, and LFDMA for CCDF of 1% are 3.6 dB, 8.0 dB, and 10.8 dB, respectively. It indicates that the PAPRs of IFDMA and LFDMA are lower by 7.2 dB and 2.8 dB, respectively, than that of OFDMA without DFT spreading [8].

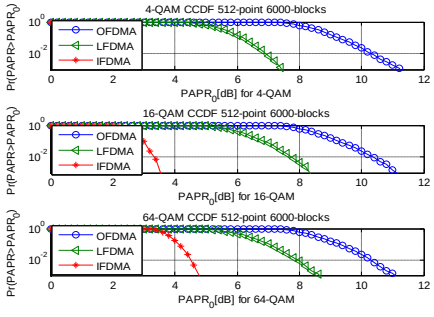

Fig 10 PAPR for IFDMA, LFDMA, and OFDMA for N= 512

ISSN: 2277-3754
ISO 9001:2008 Certified
International Journal of Engineering and Innovative Technology (IJEIT)
Volume 4, Issue 6, December 2014

Comparison of PAPR performance is shown in figure 10 when the DFT-spreading technique is applied to the IFDMA, LFDMA, and OFDMA. Different modulated signals like, 4-QAM, 16-QAM and 64 QAM are used for an SC-FDMA system with N =512, M = 64, and V = 8. Similarly, figure 11 shows a comparison of PAPR performances for CCDF of 1% when the DFT-spreading technique is applied to the IFDMA, LFDMA, and OFDMA. 4-QAM, 16-QAM and 64 QAM are used for an SC-FDMA system with N =1024, M = 64, and V = 16.

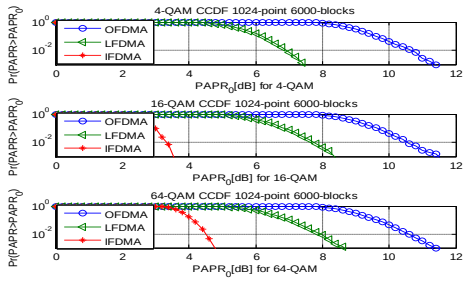

Fig 11 PAPR performances for IFDMA, LFDMA, and OFDMA for N= 1024

Table – 1 describes PAPR value of DFT - spread with 1% CCDF variation and N=256, N=512 and N=1024. It is clearly indicated that PAPR is lowest for IFDMA and highest for OFDMA. Its values increase with increase in number subcarriers and modulation type from 4- QAM to 64 – QAM.

Table-1 PAPR value of DFT- spread with 1% CCDF variation and N=256, N=512 and N=1024

Modulation Type	DFT-spread mapping	PAPR with N=256 (dB)	PAPR with N=512 (dB)	PAPR with N=1024 (dB)
4-QAM	OFDMA	10.80	11.20	11.40
	LFDMA	7.20	7.40	7.60
	IFDMA	0.02	0.04	0.06
16-QAM	OFDMA	10.80	11.00	11.40
	LFDMA	8.00	8.20	8.40
	IFDMA	3.60	3.80	4.00
64-QAM	OFDMA	10.80	11.00	11.40
	LFDMA	8.40	8.60	8.60
	IFDMA	4.60	4.80	5.00

IV. EFFECT OF PULSE SHAPING ON THE PAPR PERFORMANCE

Figure 12 shows the PAPR performance of DFT-spreading technique with IFDMA and LFDMA, when passed through a raised-Cosine pulse shaping filter with change in the value of the roll-off factor, α after IFFT operation. The impulse response of a raised cosine filter is given in equation (13).

$$s(t) = sinc\left(\Pi \frac{t}{T}\right) \frac{\cos\left(\frac{\Pi\, \alpha t}{T}\right)}{1 - \frac{4\alpha^2 t^2}{T^2}} \qquad (13)$$

Where α is the roll-off factor and its value lies between zero and 1. When value of α is low, it introduces more pulse shaping and results in more suppression of out-of-band-signal components. It can be seen from this figure that the PAPR performance of IFDMA can be significantly improved by increasing the roll-off factor from α = 0 to 1. This is in contrast with LFDMA which is not so much affected by pulse shaping. It implies that IFDMA will have a trade-off between excess bandwidth and PAPR performance since excess bandwidth increases as the roll-off factor becomes larger. The results have been obtained with the simulation parameters of N = 1024, M = 64, V = 16 and over sampling factor for pulse shaping Nos = 8 for 4- QAM signal.

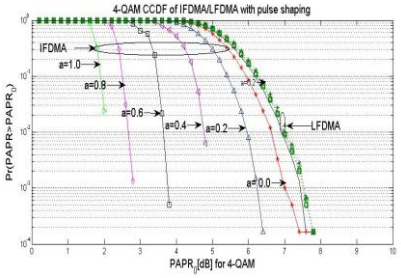

Fig 12 PAPR performances with pulse shaping filter

The PAPR performance of the LFDMA system of DFT-spreading technique is affected by the number of subcarriers M that are allocated to each user. Its PAPR performance when passed through a raised cosine pulse shaping filter is shown in figure (13) and figure (14).

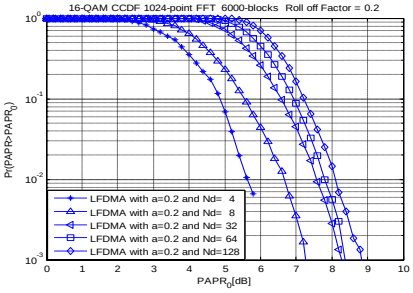

Fig 13 PAPR performance with roll- off factor = 0.2

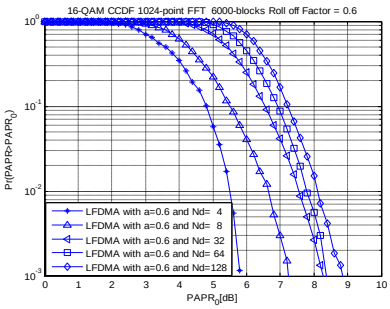

Fig 14 PAPR performance with roll- off factor = 0.6

Figure 13 shows that the PAPR performance of DFT-spreading technique for LFDMA with a roll-off factor of α = 0.2 is degraded as M increases, for example, M = 4 to 128.

ISSN: 2277-3754
ISO 9001:2008 Certified
International Journal of Engineering and Innovative Technology (IJEIT)
Volume 4, Issue 6, December 2014

Here, 64-QAM has been used for the SC-FDMA system with 1024-point FFT. Similarly, figure 13 and figure 14 shows the PAPR performance of DFT-spreading technique for LFDMA with varying M and roll-off factor, α = 0.6 and 1.0 respectively.

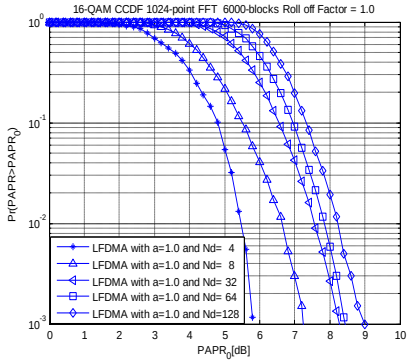

Fig 15 PAPR performance with roll- off factor = 1.0

Table-2 PAPR performance of LFDMA system with variation in sub carrier allocation

Roll-off factor, α	PAPR with M=4 (dB)	PAPR with M=8 (dB)	PAPR with M=32 (dB)	PAPR with M=64 (dB))	PAPR with M=128 (dB))
α= 0.2	5.88	7.28	8.30	8.40	8.82
α= 0.6	5.90	7.30	8.32	8.42	8.86
α= 1.0	5.92	7.32	8.34	8.44	9.00

Table -2 describes the PAPR value of LFDMA system for CCDF of 1% with variation in sub carrier allocation with constant roll- off factor, α. The change in PAPR is negligible when value of roll- off factor, α is increased from 0.2 to 1.0.

V. CONCLUSION

DFT- spread technique promises high data rate for uplink communications with lower peak to average power ratio (PAPR) than OFDM system. The PAPR obtained is almost equal to single carrier communication systems. It has benefits in terms of multipath mitigation and low-complexity equalization. IFDMA system shows sharp reduction in PAPR when applied to pulse shaping network with increase in roll-off factor from 0 to 1. The response of LFDMA is not that much affected by the pulse shaping network. For LFDMA system change in PAPR is negligible when value of roll- off factor, α is increased from 0.2 to 1.0. LFDMA is usually preferred than IFDMA from implementation point of view as subcarriers allocation with equal distance over the entire band in IFDMA system is somewhat difficult.

REFERENCES

[1] Han and Lee, "An Overview of Peak-To-Average Power Ratio Reduction Techniques for Multicarrier Transmission", IEEE Wireless Communications, April 2005.

[2] Myung, Lim, and Goodman, "Single Carrier FDMA for Uplink Wireless Transmission", IEEE Vehicular Technology Magazine, September 2006, page 30- 38.

[3] Lin, Xiao, Vucetic, and Sellathurai, "Analysis of Receiver Algorithms for LTE SC-FDMA Based Uplink MIMO Systems", IEEE Transactions on Wireless Communications, Vol. 9, No. 1, January 2010.

[4] Hasegawa, Okazaki, Kubo, Castelain, and Mottier, "A Novel PAPR Reduction Scheme for SC-OFDM with Frequency Domain Multiplexed Pilots", IEEE Communications Letters, Vol. 16, No. 9, September 2012.

[5] Berardinelli, Temiño, Frattasi, Rahman, and Mogensen, "OFDMA vs. SC-FDMA: Performance Comparison in Local Area IMT-A Scenarios", IEEE Wireless Communications • October 2008.

[6] Park and Song, "A New PAPR Reduction Technique of OFDM System with Nonlinear High Power Amplifier", IEEE Transactions on Consumer Electronics, Vol. 53, No. 2, May 2007.

[7] Priyanto, Codina, Rene, Sorensen and Mogensen, "Initial Performance Evaluation of DFT-Spread OFDM Based SC-FDMA for UTRA LTE Uplink", IEEE 65th Vehicular Technology Conference, 2007.

[8] R. Prasad, "OFDM for Wireless Communications Systems", Artech House Publishers, Norwood, MA, USA, September 2004.

[9] S. Hara and R. Prasad, "Multicarrier Techniques For 4G Mobile Communications", Artech House Publishers, Norwood, MA, USA, 2003.

[10] Cho, Kim, Yang and Kang. "MIMO- OFDM Wireless Communications with Matlab", IEEE Press, John Wiely and Sons (Asia) Pvt. Ltd., 2010.

[11] J. G. Proakis, Digital Communications, McGraw-Hill, New York, USA, Fourth edition, August 2000.

AUTHOR'S PROFILE

He is currently pursuing Ph.D. in Electronics and Communication Engineering from Gujarat Technological University, Ahmedabad. From 1986 to 2006, he was with Indian Air force. From 2006 to 2007, he worked as senior lecturer in electronics and communication engineering department at Institute of Technology, Nirma University, Ahmedabad. Since 2007, he is with the Institute of Technology and Engineering, Indus University, Ahmedabad as a head of Electrical and Electronics Engineering department. His research interest includes digital communication systems, electromagnetics, microwave and digital signal processing.

ISSN: 2277-3754
ISO 9001:2008 Certified
International Journal of Engineering and Innovative Technology (IJEIT)
Volume 4, Issue 6, December 2014

Subhash Chandra Bera received the B.Sc. degree (with honors) in physics from Presidency College, Calcutta, B. Tech. and M. Tech. degrees in radio physics and electronics from the Institute of Radio Physics and Electronics, University of Calcutta, and Ph.D. degree in Microwave Engineering from Gujarat University. Since 1994, he is with the Space Applications Centre, (ISRO), India, where he has been involved in design and development of various microwave active subsystems that are being used in many communication and navigation payload projects such as the INSAT-2, INSAT-3, INSAT-4 and GSAT of spacecraft. Presently, he is serving as head of the Satcom and navigation Systems engineering Division, Space Applications Centre, ISRO. He is Ph.D. research supervisor of Nirma University and Gujarat Technological University (GTU) in the field of Electronics and communication engineering